Journal of the Mechanics and Physics of Solids 61 (2013) 1768–1783

Contents lists available at SciVerse ScienceDirect

Journal of the Mechanics and Physics of Solids

journal homepage: www.elsevier.com/locate/jmps

Nonlinear asymptotic homogenization and the effective behavior of layered thermoelectric composites

Y. Yang [a], F.Y. Ma [a], C.H. Lei [a], Y.Y. Liu [b], J.Y. Li [a,*]

[a] Department of Mechanical Engineering, University of Washington, Seattle, WA 98195-2600, USA
[b] Faculty of Materials, Optoelectronics and Physics, and Key Laboratory of Low Dimensional Materials and Application Technology of Ministry of Education, Xiangtan University, Hunan 411105, China

ARTICLE INFO

Article history:
Received 30 July 2012
Received in revised form
5 March 2013
Accepted 23 March 2013
Available online 16 April 2013

Keywords:
Thermoelectric
Composites
Homogenization

ABSTRACT

Thermoelectric materials are promising in converting heat directly into electricity, and composite materials are often used to enhance thermoelectric figure of merit. In this work, we develop a nonlinear asymptotic homogenization theory to analyze the effective behavior of layered thermoelectric composite with coupled transport of electricity and heat. The nonlinearly coupled thermoelectric transport equations are homogenized using asymptotic analysis, from which the macroscopic field distributions are derived with local fluctuation averaged out, and overall thermoelectric conversion efficiency is established using an idealized thermoelectric module. It is discovered that the thermoelectric field distributions in the composite are different from those in a homogeneous material, and they are difficult to be fitted by homogeneous solution. Furthermore, it is noted that while the effective thermoelectric properties of the composite can be defined through a set of equivalency principle, these effective properties depend on specific boundary conditions, resulting in effective figure of merit that is not correlated with thermoelectric conversion efficiency directly. The analysis thus sheds considerable insight into the effective behavior of thermoelectric composites for their design and optimization.

1. Introduction

Thermoelectric materials are promising in converting heat directly into electricity and vice versa, and have attracted significant interests in recent years for their potential applications in waste heat recovery (Yang and Caillat, 2006; Narducci, 2011), solid state cooling and thermal management (Tritt and Subramanian, 2006), solar energy harvesting (Kraemer et al., 2011), and carbon reduction (Bell, 2008). The efficiency of thermoelectric conversion is governed by a dimensionless figure of merit ZT (Tritt et al., 2008):

$$ZT = \frac{\alpha^2 \sigma T}{\kappa}, \tag{1}$$

where α, σ, and κ are Seebeck coefficient, electric conductivity, and thermal conductivity, respectively, and T is the temperature. High thermoelectric conversion efficiency requires not only high Seebeck coefficient, but also high electric conductivity and low thermal conductivity, and this turns out to be rather difficult to achieve simultaneously, since all these properties are intimately related to each other. For example, a good electric conductor is usually a good thermal conductor

* Corresponding author. Tel.: +206 543 6226; fax: +206 685 8047.
E-mail address: jjli@u.washington.edu (J.Y. Li).

0022-5096/$ - see front matter © 2013 Elsevier Ltd. All rights reserved.
http://dx.doi.org/10.1016/j.jmps.2013.03.006

as well. As a result, one of the main strategies in developing high performance thermoelectrics is to engineer hybrid composites to enhance their conversion efficiency, especially with nanostructure engineering to take advantages of size and interface effects, and large enhancement in thermoelectric figure of merit has indeed been reported for a number of composite systems (Poudel et al., 2008; Heremans et al., 2002; Poudeu et al., 2010; Pei et al., 2011; Xie et al., 2009, 2010; Zhou et al., 2008; Zhu et al., 2009; Kim et al., 2007; Lin et al., 2005; Gothard et al., 2008; Alboni et al., 2008; Cao et al., 2008; Arachchige et al., 2008; Ke et al., 2009; Vashaee and Shakouri, 2004).

While vast amount of experimental works focus on developing thermoelectric composites, there have been only very limited theoretical efforts toward the continuum analysis of their effective behavior (Liu, 2012; Hao et al., 2012; Yang et al., 2012, 2013). Using variational principle similar to Hashin–Shtrikman bound in elasticity (Hashin and Shtrikman, 1962), it was argued that the effective figure of merit of a composite is bounded by the figure of merit of its constituents (Bergman and Levy, 1991; Bergman and Fel, 1999), though the analysis was built on linearized thermoelectric transport equations, and thus the conclusion needs to be further examined; we will come back to this point later. Furthermore, heat flux was often assumed to be divergence free (Webman et al., 1977), which is also not appropriate for thermoelectric materials with coupled transport of electricity and heat. These motivate us to examine the effective behavior of thermoelectric composites using more realistic nonlinear analysis.

As we discussed, the difficulty in continuum analysis of thermoelectric is the nonlinearly coupled electric conduction and heat transfer, which have not been sufficiently elucidated in the literature. In fact, "there is a lot of confusion, particularly in the composite materials community, as to the appropriate form of the thermoelectric equations" (Milton, 2002). Recently, we have carried out rigorous nonlinear analysis of thermoelectric transport in bilayered composite structure, where we showed that thermoelectric conversion efficiency higher than both of the constituents can be achieved (Yang et al., 2013), in contrast to the previous claim. The bilayered composite, however, is a structure without macroscopic homogeneity, and thus in this work, we analyze the thermoelectric composite with periodic microstructure, as schematically shown in Fig. 1. In Section 2, the general framework of thermoelectricity is deduced from irreversible thermodynamics, and one-dimensional field analysis is presented for homogeneous materials. Asymptotic homogenization (Bakhvalov and Panasenko, 1989; Kalamkarov et al., 2009; Triantafyllidis and Bardenhagen, 1996; Homentcovschi and Dascalu, 2000; Tarn, 1997) is then carried out in Section 3, and governing equations of coupled thermoelectric transport are homogenized. This enables us to analyze the effective behavior and conversion efficiency of the composite in Section 4, with numerical results and discussions presented in Section 5. Key observations from the analysis include the drastically different governing equations and functional distribution of thermoelectric fields in the composite from those of homogeneous materials, and the ill-defined composite figure of merit that is found to be uncorrelated with the thermoelectric conversion efficiency. Such analysis makes it possible to optimize the conversion efficiency of composite materials, which is currently undergoing.

2. Thermoelectric effects

2.1. General framework

The continuum theory of thermoelectrics can be traced back to thermodynamics, where the fundamental relation defines S, the entropy of a system, in terms of its extensive parameters internal energy U, volume V, and the mole numbers of the chemical components N_i:

$$S = S(U, V, N_i). \tag{2}$$

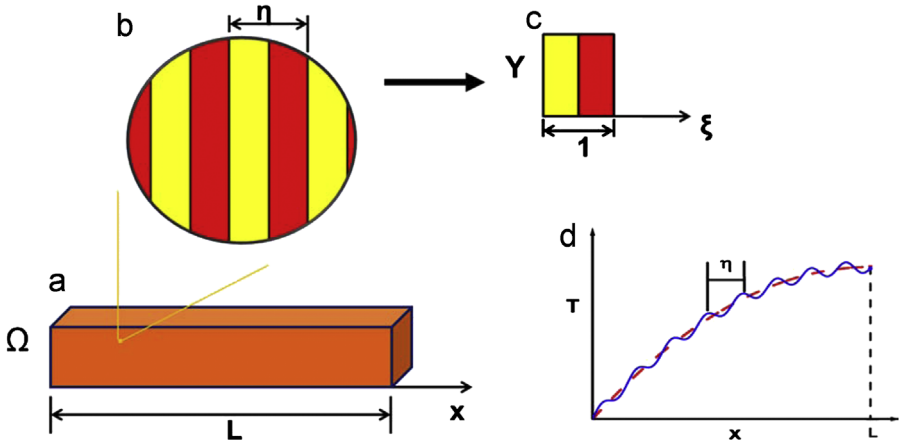

Fig. 1. Schematics of layered composite in (a) macroscopic, (b) mesoscopic, and (c) microscopic scales, with (d) fast fluctuating actual field (solid blue line) and slow varying homogenized field (dashed red line). (For interpretation of the references to color in this figure caption, the reader is referred to the web version of this article.)

We restrict ourselves to volume preserving processes, and consider electron as the only type of charge carrier, so that the fundamental relation can be recast as

$$s = s(u, n), \tag{3}$$

where s, u, and n are entropy, energy, and mole number of electrons per unit volume, respectively. By differentiating this specific fundamental relation, we derive

$$ds = \frac{1}{T}du - \frac{\mu}{T}dn, \tag{4}$$

where T is the absolute temperature, and μ is the electrochemical potential of electrons. We are particularly interested in the flows of energy and electrons, for which the rate of entropy production is evaluated as

$$\dot{s} = \nabla\frac{1}{T}\cdot\mathbf{J}_U - \nabla\frac{\mu}{T}\cdot\mathbf{J}_N, \tag{5}$$

where $\mathbf{J}_U$ and $\mathbf{J}_N$ are the fluxes of energy and electrons, respectively, while $\nabla 1/T$ and $-\nabla\mu/T$ are corresponding affinities that drive such flows. For the Markoffian system (Callen, 1960) where the fluxes depend only on the instantaneous affinities, it was proposed that

$$\begin{aligned} -\mathbf{J}_N &= L'_{11}\nabla\frac{\mu}{T} + L'_{12}\nabla\frac{1}{T}, \\ \mathbf{J}_U &= L'_{12}\nabla\frac{\mu}{T} + L'_{22}\nabla\frac{1}{T}, \end{aligned} \tag{6}$$

where isotropic symmetry is assumed for simplicity, and L'_{ij} are transport coefficients with $L'_{ij} = L'_{ji}$ due to the Onsager theorem (Callen, 1960). This set of equation is equivalent to Eq. (2.17) in Milton (2002), and it is evident that fluxes of energy and electrons are coupled by L'_{12}.

For the system we are considering, the energy is transported through both heat and electrochemical potential, and thus

$$\mathbf{J}_U = \mathbf{J}_Q + \mu\mathbf{J}_N, \tag{7}$$

where $\mathbf{J}_Q$ is the heat flux. This can be used to rewrite the transport equations as

$$\begin{aligned} -\mathbf{J}_N &= L_{11}\frac{1}{T}\nabla\mu + L_{12}\nabla\frac{1}{T}, \\ \mathbf{J}_Q &= L_{12}\frac{1}{T}\nabla\mu + L_{22}\nabla\frac{1}{T}, \end{aligned} \tag{8}$$

with

$$L_{11} = L'_{11}, \quad L_{12} = \mu L'_{11} + L'_{12}, \quad L_{22} = \mu^2 L'_{11} + 2\mu L'_{12} + L'_{22}.$$

Assume that the chemical potential of electrons is independent of temperature such that

$$\mu = e\phi, \tag{9}$$

where e is the charge of electron and ϕ is the electric potential, and notice that the electric current density $\mathbf{J}$ is related to electron flux $\mathbf{J}_N$ as

$$\mathbf{J} = e\mathbf{J}_N, \tag{10}$$

we derive the coupled transport equations for electric current density and heat flux

$$\begin{aligned} \mathbf{J} &= -\frac{e^2 L_{11}}{T}\nabla\phi + \frac{eL_{12}}{T^2}\nabla T, \\ \mathbf{J}_Q &= \frac{eL_{12}}{T}\nabla\phi - \frac{L_{22}}{T^2}\nabla T, \end{aligned} \tag{11}$$

and these are equivalent to similar equations in Milton (2002) as well. This set of transport equations allows us to establish connections between transport coefficients L_{ij} with more familiar thermoelectric properties (Goupil et al., 2011), including electric conductivity σ, thermal conductivity κ, and Seebeck coefficient α. In particular, notice that electric conductivity is measured under isothermal condition, such that

$$\sigma \equiv -\frac{J|_{\nabla T = 0}}{\nabla\phi} = \frac{e^2 L_{11}}{T}. \tag{12}$$

Similarly, thermal conductivity is measured under open-circuit condition, resulting in

$$\kappa \equiv = -\frac{J_Q|_{J=0}}{\nabla T} = \frac{L_{11}L_{22} - L_{12}^2}{T^2 L_{11}}. \tag{13}$$

Furthermore, Seebeck coefficient is measured as electric field induced by unit temperature gradient, under open-circuit condition, leading to

$$\alpha \equiv -\frac{\nabla\phi|_{J=0}}{\nabla T} = -\frac{L_{12}}{eTL_{11}}. \tag{14}$$

With these connections, the thermoelectric transport equations can then be recast into more familiar form as

$$\begin{aligned} -\mathbf{J} &= \sigma\nabla\phi + \sigma\alpha\nabla T, \\ \mathbf{J}_Q &= -T\alpha\sigma\nabla\phi - (T\alpha^2\sigma + \kappa)\nabla T = T\alpha\mathbf{J} - \kappa\nabla T, \end{aligned} \tag{15}$$

which are nonlinearly coupled due to the terms $T\nabla\phi$ and $T\nabla T$. In the absence of thermoelectric effect where $\alpha = 0$, the uncoupled transport equations of electricity and heat are recovered.

It is also evident from energy transport that

$$\mathbf{J}_U = \mathbf{J}_Q + \phi\mathbf{J}, \tag{16}$$

and for a system wherein both charges and energy are conserved, current density and energy flux are divergence-free,

$$\begin{aligned} \nabla\cdot\mathbf{J} &= 0, \\ \nabla\cdot\mathbf{J}_U &= 0, \end{aligned} \tag{17}$$

while the heat flux is no longer divergence-free in general,

$$\nabla\cdot\mathbf{J}_Q = -\nabla\cdot(\phi\mathbf{J}) = -\nabla\phi\cdot\mathbf{J}, \tag{18}$$

where Joule heat serves as heat source. This is in contrast to a normal heat transfer problem uncoupled from electric conduction.

Before we proceed, we make the following observations on various forms of constitutive equations, (6), (8), (11) and (15). They of course are all equivalent, yet subtle difference exists. The first set of equations, (6), appears to be linear, if the involved kinetic coefficients L'_{ij} can be viewed as constants independent of temperature and electrochemical potential; these would make homogenization straightforward (Milgrom and Shtrikman, 1989; Milton, 2002). Indeed, as recently pointed out by Liu (2012), these kinetic coefficients can be regarded as constants under small deviation of the temperature and electrochemical potential from their equilibrium values, with which the transport equations can be linearized. However, under more general circumstances, these kinetic coefficients are functions of local intensive parameters (Callen, 1960), and thus cannot be viewed as constants, making the governing equation intrinsically nonlinear. These can be better appreciated from Eq. (12). If $L'_{11} = L_{11} = \sigma T/e^2$ would be a constant independent of temperature, then the electric conductivity σ would vary inversely with respect to temperature, as noted by Liu (2012). For semiconductors that most good thermoelectrics belong to, it is well known that the intrinsic electric conductivity generally increases with respect to temperature. In fact, electric conductivity, thermal conductivity, and Seebeck coefficient all have complicated variation with respect to temperature, and thus thermoelectric transport equations have to be regarded as nonlinear in general. Eq. (6) also appears to be advantageous compared to the other three sets of equations in that both $\mathbf{J}_N$ and $\mathbf{J}_U$ are divergence-free, yet the physical meanings of the corresponding kinetic coefficients are less straightforward. In this work, we choose to work with Eq. (15), for its close connection with widely used thermoelectric properties. It is worth noting that Eq. (15) is essentially identical to the transport equations used by Bergman and Levy (1991) and Bergman and Fel (1999), who linearized the equations by treating $\kappa/T + \sigma\alpha^2$ as a constant, making it possible to use Hashin–Shtrikman variational principle to bound the effective figure of merit of thermoelectric composite. As pointed out by Liu (2012), this would also require small deviation of temperature and electrochemical potential from their equilibrium values. Furthermore, the linearized version of Eqs. (6) and (15) are no longer equivalent, and their solutions to specific problems are different. In this work, we do not invoke these assumptions for linearization, and will examine the implication of nonlinearity in the transport equations to the thermoelectric properties of composites.

2.2. One-dimensional system

To be specific, we confine our scope to one-dimensional (1D) system in this work, wherein all the field variables and materials parameters are assumed to be dependent only on coordinate x, and independent of y and z, and the thermoelectric transport equations are simplified as

$$-J = \sigma\frac{d\phi}{dx} + \sigma\alpha\frac{dT}{dx}, \tag{19}$$

$$J_Q = \alpha TJ - \kappa\frac{dT}{dx}. \tag{20}$$

In addition, the divergence-free of current density implies that $J = |\mathbf{J}| = const$ in 1D, and the field equation for heat flux is simplified as

$$\frac{dJ_Q}{dx} = -\frac{d\phi}{dx}J. \tag{21}$$

The transport equations can be combined with the field equation, resulting in the following governing equations for temperature and electric potential in a homogeneous medium wherein all the thermoelectric properties are constant,

$$\frac{d^2T}{dx^2}+\frac{1}{\sigma\kappa}J^2=0, \tag{22}$$

$$\frac{d^2\phi}{dx^2}-\frac{\alpha}{\sigma\kappa}J^2=0, \tag{23}$$

resulting in quadratic distribution of temperature and potential

$$T(x)=-\frac{J^2}{2\sigma\kappa}x^2+k_1x+k_2, \tag{24}$$

$$\phi(x)=\frac{\alpha J^2}{2\sigma\kappa}x^2-\left(\frac{J}{\sigma}+\alpha k_1\right)x+k_3, \tag{25}$$

and a constant current density

$$J=\frac{-\sigma\alpha[T(L)-T(0)]-\sigma[\phi(L)-\phi(0)]}{L}, \tag{26}$$

with

$$k_1=\frac{[T(L)-T(0)]}{L}+\frac{J^2L}{2\sigma\kappa},\quad k_2=T(0),\quad k_3=\phi(0), \tag{27}$$

where $T(x)$ and $\phi(x)$ at $x=0,L$ are specified as the boundary conditions. The heat flux is then calculated as

$$J_Q(x)=-\frac{\alpha J^3}{2\sigma\kappa}x^2+\left(\frac{J^2}{\sigma}+\alpha Jk_1\right)x-\kappa k_1+\alpha Jk_2. \tag{28}$$

For bilayered thermoelectric composites consisting of two different materials with distinct thermoelectric properties, analytic solutions have also been obtained (Yang et al., 2012). In this work, however, we are interested in layered composites with periodic microstructure, which we approach using asymptotic analysis, as we discuss next.

3. Asymptotic homogenization

We consider a 1D composite consisting of two distinct phases layered periodically, as schematically shown in Fig. 1. For such a composite, two different length scales can be identified, one is L, the macroscopic length of the composite associated with the macroscopic coordinate x. The other is η, the characteristic length of the composite unit cell, for which a microscopic coordinate $\xi=x/\eta$ can be introduced. While the material properties $\alpha(\xi)$, $\sigma(\xi)$, and $\kappa(\xi)$ vary fast on the microscopic scale periodically, the field variables such as $T(x,\xi)$, $\phi(x,\xi)$, and $J_Q(x,\xi)$ vary both fast on microscopic scale and slowly on macroscopic scale, as schematically shown in Fig. 1(d). What we are interested in is the macroscopic variation of these field variables, for which the fast microscopic fluctuation is averaged out, so that the effective behavior of the composite can be deduced.

To this end, we expand the temperature, potential, and heat flux into polynomials of η

$$T(x,\xi)=T_0(x,\xi)+\eta T_1(x,\xi)+\eta^2T_2(x,\xi)+\cdots, \tag{29}$$

$$\phi(x,\xi)=\phi_0(x,\xi)+\eta\phi_1(x,\xi)+\eta^2\phi_2(x,\xi)+\cdots, \tag{30}$$

$$J_Q(x,\xi)=J_{Q0}(x,\xi)+\eta J_{Q1}(x,\xi)+\eta^2J_{Q2}(x,\xi)+\cdots \tag{31}$$

Inserting these into governing Eqs. (19) and (21) for T and ϕ, and noticing that

$$\frac{d}{dx}\to\frac{\partial}{\partial x}+\frac{1}{\eta}\frac{\partial}{\partial\xi}, \tag{32}$$

we obtain a series of equations grouped by the orders of η as following:

$$\eta^{-2}:\ \frac{\partial}{\partial\xi}\left(\kappa\frac{\partial T_0}{\partial\xi}\right)=0, \tag{33}$$

$$\eta^{-1}:\ \sigma\frac{\partial\phi_0}{\partial\xi}+\sigma\alpha\frac{\partial T_0}{\partial\xi}=0, \tag{34}$$

$$\frac{\partial}{\partial x}\left(\kappa\frac{\partial T_0}{\partial\xi}\right)+\frac{\partial}{\partial\xi}\left(-\alpha JT_0+\kappa\frac{\partial T_0}{\partial x}+\kappa\frac{\partial T_1}{\partial\xi}\right)=\frac{\partial\phi_0}{\partial\xi}J, \tag{35}$$

$$\eta^{-0}:\ -J=\sigma\left(\frac{\partial\phi_0}{\partial x}+\frac{\partial\phi_1}{\partial\xi}\right)+\sigma\alpha\left(\frac{\partial T_0}{\partial x}+\frac{\partial T_1}{\partial\xi}\right), \tag{36}$$

$$\left(\frac{\partial\phi_0}{\partial x}+\frac{\partial\phi_1}{\partial\xi}\right)J=\frac{\partial}{\partial x}\left(-\alpha JT_0+\kappa\frac{\partial T_0}{\partial x}+\kappa\frac{\partial T_1}{\partial\xi}\right)+\frac{\partial}{\partial\xi}\left(-\alpha JT_1+\kappa\frac{\partial T_1}{\partial x}+\kappa\frac{\partial T_2}{\partial\xi}\right). \tag{37}$$

We first examine $T_0(x,\xi)$ and $\phi_0(x,\xi)$, the lowest order of field variables. By integrating Eq. (33) and rearranging the equation, we obtain

$$\frac{\partial T_0}{\partial\xi}=\frac{C_1(x)}{\kappa(\xi)}. \tag{38}$$

Since $T_0(x,\xi)$ is periodic in ξ, and the integration of $\partial T_0/\partial\xi$ over the unit cell vanishes, it is concluded that $C_1(x)=0$, and thus

$$T_0(x,\xi)=T_0(x). \tag{39}$$

Combining this with Eq. (34), it is also evident that

$$\phi_0(x,\xi)=\phi_0(x). \tag{40}$$

In other words, $T_0(x)$ and $\phi_0(x)$ do not vary on microscopic scale, and they represent the macroscopic distributions of temperature and potential when $\eta\to 0$. They thus describe the effective behavior of the layered composite with local fluctuations of temperature and potential averaged out, which we seek to determine.

We then examine $T_1(x,\xi)$ and $\phi_1(x,\xi)$. Making use of Eqs. (39) and (40), we can integrate Eq. (35) with respect to ξ as

$$\frac{\partial T_1}{\partial\xi}=-\frac{dT_0}{dx}+\frac{\alpha(\xi)}{\kappa(\xi)}JT_0(x)+\frac{C_2(x)}{\kappa(\xi)}, \tag{41}$$

with

$$C_2=\langle\frac{1}{\kappa}\rangle^{-1}\left(\frac{dT_0}{dx}-\langle\frac{\alpha}{\kappa}\rangle JT_0\right) \tag{42}$$

determined again from the periodicity of $T_1(x,\xi)$ on the unit cell, where $\langle\cdot\rangle$ is used to indicate volume averaged quantities over the unit cell. Integrating Eq. (41) one more time, we obtain

$$T_1(x,\xi)=\frac{dT_0}{dx}\int_0^\xi\left(\kappa^{-1}\langle\frac{1}{\kappa}\rangle^{-1}-1\right)d\xi-JT_0\int_0^\xi\left(\kappa^{-1}\langle\frac{1}{\kappa}\rangle^{-1}\langle\frac{\alpha}{\kappa}\rangle-\frac{\alpha}{\kappa}\right)d\xi, \tag{43}$$

for which the integration constant $C_3(x)$ is assumed to be zero without loss of generality, since it can be incorporated into $T_0(x)$. Similarly, Eq. (36) can be recast as

$$\frac{\partial\phi_1}{\partial\xi}=-\frac{J}{\sigma}-\frac{d\phi_0}{dx}-\frac{\alpha}{\kappa}\langle\frac{1}{\kappa}\rangle^{-1}\frac{dT_0}{dx}+\left(\frac{\alpha}{\kappa}\langle\frac{1}{\kappa}\rangle^{-1}\langle\frac{\alpha}{\kappa}\rangle-\frac{\alpha^2}{\kappa}\right)JT_0, \tag{44}$$

which by integration yields

$$\phi_1(x,\xi)=-J\int_0^\xi\frac{1}{\sigma}d\xi-\frac{d\phi_0}{dx}\xi-\frac{dT_0}{dx}\int_0^\xi\frac{\alpha}{\kappa}\langle\frac{1}{\kappa}\rangle^{-1}d\xi+JT_0\int_0^\xi\left(\frac{\alpha}{\kappa}\langle\frac{1}{\kappa}\rangle^{-1}\langle\frac{\alpha}{\kappa}\rangle-\frac{\alpha^2}{\kappa}\right)d\xi. \tag{45}$$

As such, Eqs. (43) and (45), respectively, give $T_1(x,\xi)$ and $\phi_1(x,\xi)$ that fluctuate fast on the microscopic scale on the order of η. This will be sufficient for our analysis, and higher order fluctuations will not be considered.

In order to derive the governing equations for $T_0(x)$ and $\phi_0(x)$ that describe the effective behavior of the layered composite, we integrate Eq. (37) over the unit cell to obtain

$$\int_0^1\frac{\partial}{\partial x}\left(-\alpha JT_0+\kappa\frac{\partial T_0}{\partial x}+\kappa\frac{\partial T_1}{\partial\xi}\right)d\xi=\int_0^1\left(\frac{\partial\phi_0}{\partial x}+\frac{\partial\phi_1}{\partial\xi}\right)J\,d\xi, \tag{46}$$

which can be simplified by using Eqs. (41), (42), and (44), resulting in

$$\frac{d^2T_0}{dx^2}+\langle\frac{1}{\sigma}\rangle\langle\frac{1}{\kappa}\rangle J^2-\left(\langle\frac{\alpha}{\kappa}\rangle^2-\langle\frac{\alpha^2}{\kappa}\rangle\langle\frac{1}{\kappa}\rangle\right)J^2T_0=0. \tag{47}$$

This is the governing equation for the macroscopic temperature distribution $T_0(x)$ in the layered composite. Furthermore, we integrate Eq. (44) over the unit cell to obtain

$$\frac{d\phi_0}{dx}=-\langle\frac{1}{\sigma}\rangle J-\langle\frac{\alpha}{\kappa}\rangle\langle\frac{1}{\kappa}\rangle^{-1}\frac{dT_0}{dx}+\left(\langle\frac{1}{\kappa}\rangle^{-1}\langle\frac{\alpha}{\kappa}\rangle^2-\langle\frac{\alpha^2}{\kappa}\rangle\right)JT_0. \tag{48}$$

By combining Eqs. (42) and (48), we can rewrite C_2 as

$$C_2=-\langle\frac{\alpha}{\kappa}\rangle^{-1}\left(\frac{d\phi_0}{dx}+\langle\frac{\alpha^2}{\kappa}\rangle JT_0+\langle\frac{1}{\sigma}\rangle J\right), \tag{49}$$

which can be used to recast Eq. (46) as

$$\frac{d^2\phi_0}{dx^2}-\langle\frac{1}{\sigma}\rangle\langle\frac{\alpha}{\kappa}\rangle J^2+\left(\langle\frac{\alpha^2}{\kappa}\rangle-\langle\frac{\alpha}{\kappa}\rangle^2\langle\frac{1}{\kappa}\rangle^{-1}\right)J\frac{dT_0}{dx}-\left(\langle\frac{\alpha^2}{\kappa}\rangle\langle\frac{\alpha}{\kappa}\rangle-\langle\frac{\alpha}{\kappa}\rangle^3\langle\frac{1}{\kappa}\rangle^{-1}\right)J^2T_0=0. \tag{50}$$

This is the governing equation for the macroscopic potential distribution $\phi_0(x)$ in the layered composite.

Eqs. (47) and (50) are homogenized governing equations for temperature and potential distribution in layered periodic composite, one of the key results in this work, and the coefficients in these equations can be easily determined from the volume averages of appropriate quantities in the unit cell. These homogenized governing equations are considerably more complicated than those of homogeneous materials, Eqs. (22) and (23), a consequence of nonlinearly coupled transport equations (Agoras et al., 2009; Ghosh et al., 2009), and it is easy to verify that under limiting case of homogeneous materials, the homogeneous governing equations are recovered. With $T_0(x)$ and $\phi_0(x)$ solved from Eqs. (47) and (50), the macroscopic distribution of heat flux can be derived as

$$J_{Q0}=\langle\frac{1}{\kappa}\rangle^{-1}\left(\langle\frac{\alpha}{\kappa}\rangle T_0J-\frac{dT_0}{dx}\right), \tag{51}$$

where Eqs. (41) and (42) have been used. Thus the problem is completely solved, if we can determine the macroscopic temperature and potential distributions along with the constant current density, which we seek to solve in the next section. We can further determine the local fluctuations of temperature and potential from Eqs. (43) and (45), though we are more interested in the effective behavior, and this line of investigation will not be pursued here.

4. The effective behavior

4.1. Field analysis

In order to solve for the temperature distribution in the layered composite, we recast Eq. (47), a second order ordinary differential equation with constant coefficients, as

$$\frac{d^2T_0}{dx^2}+d_1T_0+d_2=0, \tag{52}$$

with

$$d_1=\left(\langle\frac{\alpha^2}{\kappa}\rangle\langle\frac{1}{\kappa}\rangle-\langle\frac{\alpha}{\kappa}\rangle^2\right)J^2,\quad d_2=\langle\frac{1}{\sigma}\rangle\langle\frac{1}{\kappa}\rangle J^2,$$

which can be solved as

$$T_0(x)=q_1\cos(\sqrt{d_1}x)+q_2\sin(\sqrt{d_1}x)-\frac{d_2}{d_1}, \tag{53}$$

where q_1 and q_2 are constants that can be determined by boundary conditions as

$$q_1=\frac{d_2}{d_1}+T(0),\quad q_2=\frac{d_2/d_1+T(L)-q_1\cos(\sqrt{d_1}L)}{\sin(\sqrt{d_1}L)}. \tag{54}$$

Not surprisingly, the functional variation of macroscopic temperature distribution of the layered composite is drastically different from the quadratic distribution of homogeneous materials in Eq. (24). Having derived $T_0(x)$, we can solve for $\phi_0(x)$ from Eq. (48) in a similar manner as

$$\phi_0=h_1x+h_2\sin(\sqrt{d_1}x)+h_3\cos(\sqrt{d_1}x)+h_4, \tag{55}$$

with

$$h_1=-\langle\frac{1}{\sigma}\rangle J-\left(\langle\frac{1}{\kappa}\rangle^{-1}\langle\frac{\alpha}{\kappa}\rangle^2-\langle\frac{\alpha^2}{\kappa}\rangle\right)J\frac{d_2}{d_1},$$

$$h_2=-\langle\frac{1}{\kappa}\rangle^{-1}\langle\frac{\alpha}{\kappa}\rangle q_2+\left(\langle\frac{1}{\kappa}\rangle^{-1}\langle\frac{\alpha}{\kappa}\rangle^2-\langle\frac{\alpha^2}{\kappa}\rangle\right)J\frac{q_1}{\sqrt{d_1}},$$

$$h_3=-\langle\frac{1}{\kappa}\rangle^{-1}\langle\frac{\alpha}{\kappa}\rangle q_1-\left(\langle\frac{1}{\kappa}\rangle^{-1}\langle\frac{\alpha}{\kappa}\rangle^2-\langle\frac{\alpha^2}{\kappa}\rangle\right)J\frac{q_2}{\sqrt{d_1}},$$

$$h_4=\phi(0)-h_3.$$

Note that both temperature and potential distributions are given in terms of yet to be determined current density J, which can be solved from potential boundary condition at $x=L$,

$$\phi_0(L) = h_1 L + h_2 \sin(\sqrt{d_1}L) + h_3 \cos(\sqrt{d_1}L) + h_4. \tag{56}$$

With the current density J determined as such, the heat and energy fluxes can be determined accordingly,

$$J_{Q0} = -\langle\frac{1}{\kappa}\rangle^{-1}\left[\left(-q_1\sqrt{d_1}-\langle\frac{\alpha}{\kappa}\rangle J q_2\right)\sin(\sqrt{d_1}x)+(q_2\sqrt{d_1}-\langle\frac{\alpha}{\kappa}\rangle J q_1)\cos(\sqrt{d_1}x) + \langle\frac{\alpha}{\kappa}\rangle J\frac{d_2}{d_1}\right], \tag{57}$$

and

$$J_U = \langle\frac{1}{\kappa}\rangle^{-1}\left(\langle\frac{\alpha}{\kappa}\rangle T_0 J - \frac{dT_0}{dx}\right) + \phi_0 J. \tag{58}$$

This set of equations completely solved the macroscopic variation of temperature, potential, current density, heat flux, and energy flux in a layered composite, and thus completely describe its effective behavior.

4.2. The effective properties

The effective behavior of a composite material can often be described in terms of its effective constitutive constants, and this can also be attempted for thermoelectric composite. Since the effective properties of a nonlinear composite depends on the given boundary condition, we define the effective thermoelectric properties through the following equivalency principle (Yang et al., 2012). Given the identical boundary conditions of temperature and electric potential, a thermoelectric composite with a set of effective thermoelectric properties should have identical current density and energy flux as a homogeneous thermoelectric with the same set of properties. With such equivalency, it is clear that the composite and homogeneous thermoelectrics can be exchanged under the specified boundary conditions.

With such equivalency principle, we examine the effective electric conductivity first. Consider a boundary condition of imposed electric potential difference only with $\Delta T = 0$, and compare the current density between homogeneous thermoelectric and periodic composite, we conclude that the effective electric conductivity of the periodic composite is given by

$$\sigma^*(\Delta\phi, \Delta T = 0) = -\frac{J}{\Delta\phi/L}, \tag{59}$$

with the current density determined by Eq. (56). Since $\Delta T = 0$, the current density can be solved analytically, resulting in

$$\sigma^* = \frac{2}{v\Delta\phi}\tan^{-1}\left\{\frac{\langle\frac{1}{\kappa}\rangle v\Delta\phi}{2\left[\langle\frac{1}{\sigma}\rangle\langle\frac{1}{\kappa}\rangle + v^2 T(0)\right]}\right\}, \tag{60}$$

with

$$v = \sqrt{\langle\frac{\alpha^2}{\kappa}\rangle\langle\frac{1}{\kappa}\rangle - \langle\frac{\alpha}{\kappa}\rangle^2}.$$

Clearly, the effective electric conductivity depends on the imposed potential difference at boundary in addition to the material constants of the constituents and the volume fraction f, a characteristic distinct from linear medium. On the other hand, if we impose open-circuit boundary condition where $J=0$, such that

$$\frac{d\phi_0}{dx} = -\langle\frac{\alpha}{\kappa}\rangle\langle\frac{1}{\kappa}\rangle^{-1}\frac{dT_0}{dx}, \tag{61}$$

the effective Seebeck coefficient can be derived as

$$\alpha^* = -\frac{\phi(L)-\phi(0)}{T(L)-T(0)} = \langle\frac{\alpha}{\kappa}\rangle\langle\frac{1}{\kappa}\rangle^{-1}. \tag{62}$$

In addition, under the condition of $J=0$, we have

$$J_{Q0} = -\langle\frac{1}{\kappa}\rangle^{-1}\frac{dT_0}{dx}, \tag{63}$$

from which the effective thermal conductivity can be derived as

$$\kappa^* = -\frac{J_{Q0}}{[T(L)-T(0)]/L} = \langle\frac{1}{\kappa}\rangle^{-1}. \tag{64}$$

Notice that this effective thermal conductivity is identical to that of a layered linear thermal conductor uncoupled from electric conduction, since open circuit condition is assumed, and different effective Seebeck coefficient and thermal conductivity will be resulted if different electric boundary condition is imposed. From these effective thermoelectric

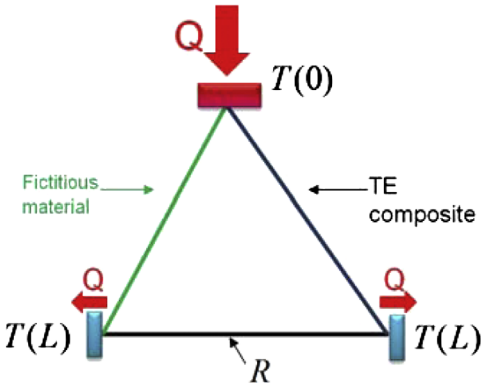

Fig. 2. Schematics of the fictitious thermoelectric module for conversion efficiency analysis.

properties, the effective thermoelectric figure of merit is then defined as

$$Z^* = \frac{\sigma^* \alpha^{*2}}{\kappa^*}, \tag{65}$$

though its connection with the thermoelectric conversion efficiency remains to be examined, which we analyze in the next subsection.

4.3. Thermoelectric conversion efficiency

While the figure of merit is directly related to thermoelectric conversion efficiency for a homogeneous material, our analysis on bilayered thermoelectric composite indicates that it is not well defined for heterogeneous thermoelectric. As a result, we analyze the thermoelectric conversion efficiency of the periodic layered composite directly, based on the thermoelectric module schematically shown in Fig. 2. One leg of the module is made of material of interest, which is the layered composite with periodic microstructure, and the other leg is made of a fictitious material with zero Seebeck coefficient and thermal conductivity, yet infinite electric conductivity, and thus it only serves as a path for electric current, not involved in energy conversion. The conversion efficiency of this idealized thermoelectric module, as a result, measures only the performance of the composite material of interest, and it can be defined as

$$H = \frac{(JA)^2 R}{\dot{E}_0} = \frac{(JA)^2 R}{A J_U|_{x=0}}, \tag{66}$$

where the numerator denotes the electric energy delivered to the load resistance, whereas the denominator denotes the heat (energy) flowing in at the joint from the hot reservoir with temperature $T(0)$. From Eq. (58), it is derived that

$$J_U|_{x=0} = \langle \frac{1}{\kappa} \rangle^{-1} \left[\langle \frac{\alpha}{\kappa} \rangle T(0) J - \frac{dT_0}{dx}|_{x=0} \right], \tag{67}$$

and the current density J can be determined from integral of $\nabla\phi$ around the circuit,

$$\oint \nabla\phi \cdot d\mathbf{r} = 0, \tag{68}$$

which replaces the imposed potential at boundaries we used earlier. The efficiency can be optimized with respect to the load resistance R, and for homogeneous materials, this lead to classical equation relating figure of merit ZT to optimal conversion efficiency under given temperature difference,

$$H_{\text{opt}} = \frac{T_h - T_c}{T_h} \frac{\sqrt{1 + Z\frac{T_h + T_c}{2}} - 1}{\sqrt{1 + Z\frac{T_h + T_c}{2}} + \frac{T_c}{T_h}}, \tag{69}$$

where T_h and T_c refer to temperatures at hot and cold ends, respectively. For composite materials, however, such simple relationship is no longer available, and we have to evaluate the optimal conversion efficiency numerically in general. Alternatively, it is sometimes insightful to recast the conversion efficiency as

$$H = \frac{\phi(L) J}{J_U|_{x=0}} = \frac{\phi(L) J}{\langle \frac{1}{\kappa} \rangle^{-1} \left(\langle \frac{\alpha}{\kappa} \rangle T(0) J - \frac{dT_0}{dx}\Big|_{x=0} \right)}, \tag{70}$$

with

$$\phi(L) = -\langle \frac{1}{\sigma} \rangle JL - \langle \frac{\alpha}{\kappa} \rangle \langle \frac{1}{\kappa} \rangle^{-1} [T(L) - T(0)] + \left(\langle \frac{1}{\kappa} \rangle^{-1} \langle \frac{\alpha}{\kappa} \rangle^2 - \langle \frac{\alpha^2}{\kappa} \rangle \right) J \int_0^L T_0 \, dx, \tag{71}$$

where $\phi(0) = 0$ is assumed without loss of generality. The efficiency can then be optimized equivalently with respect to the current density instead, though the current density is upper bounded by the current density achieved without the load resistance. These two approaches for deriving the optimal conversion efficiency are equivalent, and both requires numerical computation in general, yet the one using current density is more efficient numerically.

5. Results and discussions

5.1. Field distributions

To demonstrate the analysis, we consider a periodic thermoelectric composite consisting of Bi_2Te_3 and $Ag(Pb_{1-y}Sn_y)_mSbTe_{2+m}$, with their thermoelectric properties listed in Table 1 and the volume fraction of Bi_2Te_3 being f.

Table 1
Thermoelectric properties of Bi_2Te_3 (Antonova and Looman, 2005) and $Ag(Pb_{1-y}Sn_y)_mSbTe_{2+m}$ (Androulakis et al., 2006).

Material	α ($\times 10^{-6}$ V/K)	σ ($\times 10^3$ S/m)	κ (W/m/K)
Bi_2Te_3	200	110	1.6
$Ag(Pb_{1-y}Sn_y)_mSbTe_{2+m}$	270	22	0.77

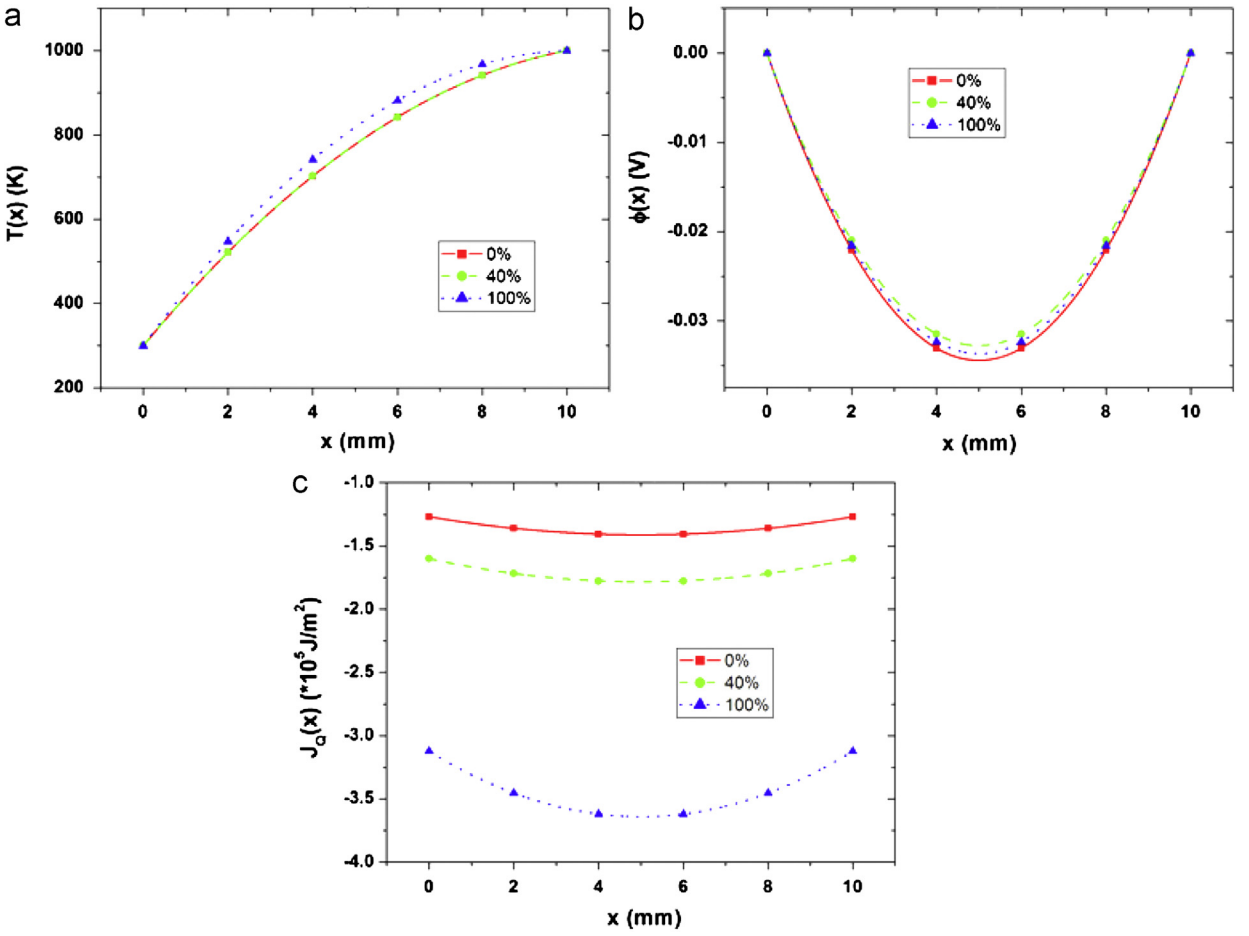

Fig. 3. The distributions of (a) temperature, (b) electric potential, and (c) heat flux in thermoelectric composite under an imposed temperature difference of $T(0) = 300$ K and $T(L) = 1000$ K, with $\phi(0) = \phi(L) = 0$ and $f = 0, 0.4, 1$.

Notice that both phases have excellent Seebeck coefficient that are comparable to each other, yet Bi_2Te_3 has relatively high thermal conductivity, while $Ag(Pb_{1-y}Sn_y)_mSbTe_{2+m}$ has relatively low electric conductivity, both of which are not desirable for high thermoelectric conversion efficiency. Consider either only a temperature difference or an electric potential difference is imposed, and the corresponding distributions of temperature, electric potential, and heat flux are shown in Figs. 3 and 4, where $f=0.4$ is assumed, and homogeneous materials with $f=0$, 1 are also included for comparison. It is observed that under both types of boundary conditions, the field distributions are highly nonlinear, as expected, and the heat flux is not constant. Notable temperature rising is also observed in Fig. 4 inside of the composite under imposed potential difference, due to Joule heating, and the increase in temperature is most prominent in Bi_2Te_3, which has higher electric conductivity, and its heat flux is also larger due to higher thermal conductivity.

It is worth noting that the quantitative variations of temperature and electric potential for the layered composite are not much different from those of homogeneous materials, despite drastically different functional forms. This motivates us to fit the distributions of temperature, potential, or the heat flux in the composite using homogeneous solutions, Eqs. (24), (25), and (28). The resulting sets of thermoelectric properties identified from these fittings are listed in Table 2, where it is observed that different curves resulting in thermoelectric constants that differ in orders of magnitude, for both types of boundary conditions. In other words, it is difficult to identify a consistent set of effective thermoelectric properties that fit the distributions of temperature, potential, and heat flux simultaneously under given boundary conditions. The comparison of original distributions and fitted results shown in Figs. 5 and 6 also confirm this observation. For example, in Fig. 5, it is observed that the data fitted by heat flux leads to good agreement for temperature distribution, yet results in poor agreement for potential. In Fig. 6, on the other hand, the data fitted by heat flux results in poor agreement for both temperature and potential. Similar conclusion can be drawn for data fitted by temperature or potential. This highlights the difficulty in homogenizing the effective thermoelectric properties of the composite that would resemble the behavior of homogeneous materials.

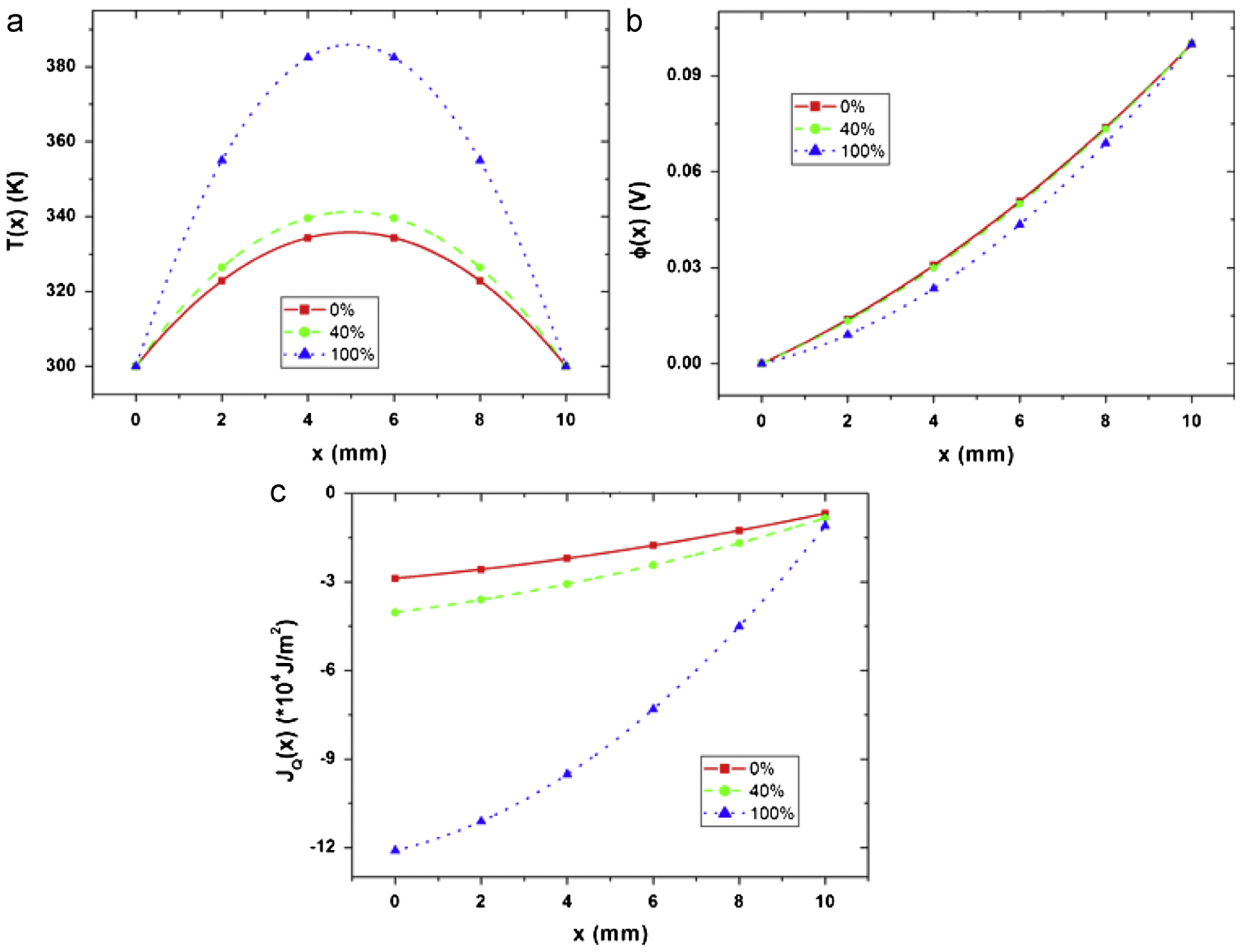

Fig. 4. The distributions of (a) temperature, (b) electric potential, and (c) heat flux in thermoelectric composite under an imposed electric potential difference of $\phi(0)=0$ and $\phi(L)=0.1$ V, with $T(0)=T(L)=300$ K and $f=0, 0.4, 1$.

5.2. The effective properties and conversion efficiency

Since it is impossible to find a set of effective thermoelectric properties of composite that will fit its distributions of temperature, potential, and heat flux into homogeneous solution, we calculate the effective properties of the composite versus the volume fraction of Bi_2Te_3 using equivalency principle instead, as shown in Fig. 7, which ensures the equivalency in current density and energy flux between composite and homogeneous material with the identical set of properties. The effective Seebeck coefficient and thermal conductivity are calculated under open circuit condition, and the effective electric conductivity is evaluated with $T(0)=T(L)=300$ K and $\Delta\phi=0.2, 0.35, 0.5, 1.0$ K. It is observed that there is a noticeable

Table 2
By fitting curves of temperature, electric potential, and heat flux of composite to homogeneous results, sets of thermoelectric properties are derived.

Curves fitted	α ($\times10^{-6}$ V/K)	σ ($\times10^{4}$ S/m)	κ (W/m/K)
Under imposed ΔT:			
T_0	541	635	890
ϕ_0	467	440	838
J_{Q0}	29 077	0.0002	1
Under imposed $\Delta\phi$:			
T_0	2424	3156	957
ϕ_0	1016	809	985
J_{Q0}	276	3	620

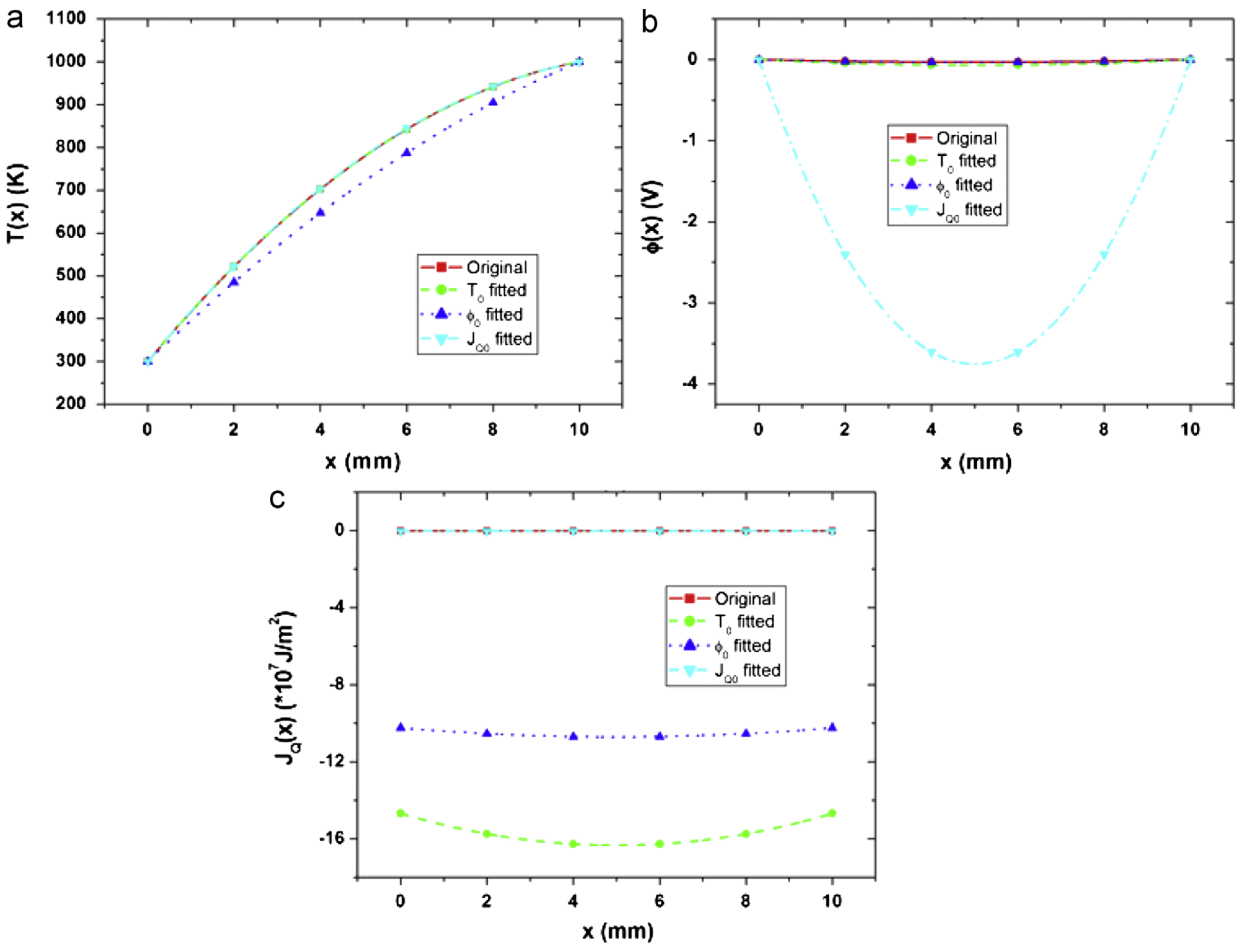

Fig. 5. Distribution of (a) temperature, (b) electric potential, and (c) heat flux of thermoelectric composite are fitted to the solutions of homogeneous material for $T(0)=300$ K, $T(L)=1000$ K, $\phi(0)=\phi(L)=0$, and $f=0.4$.

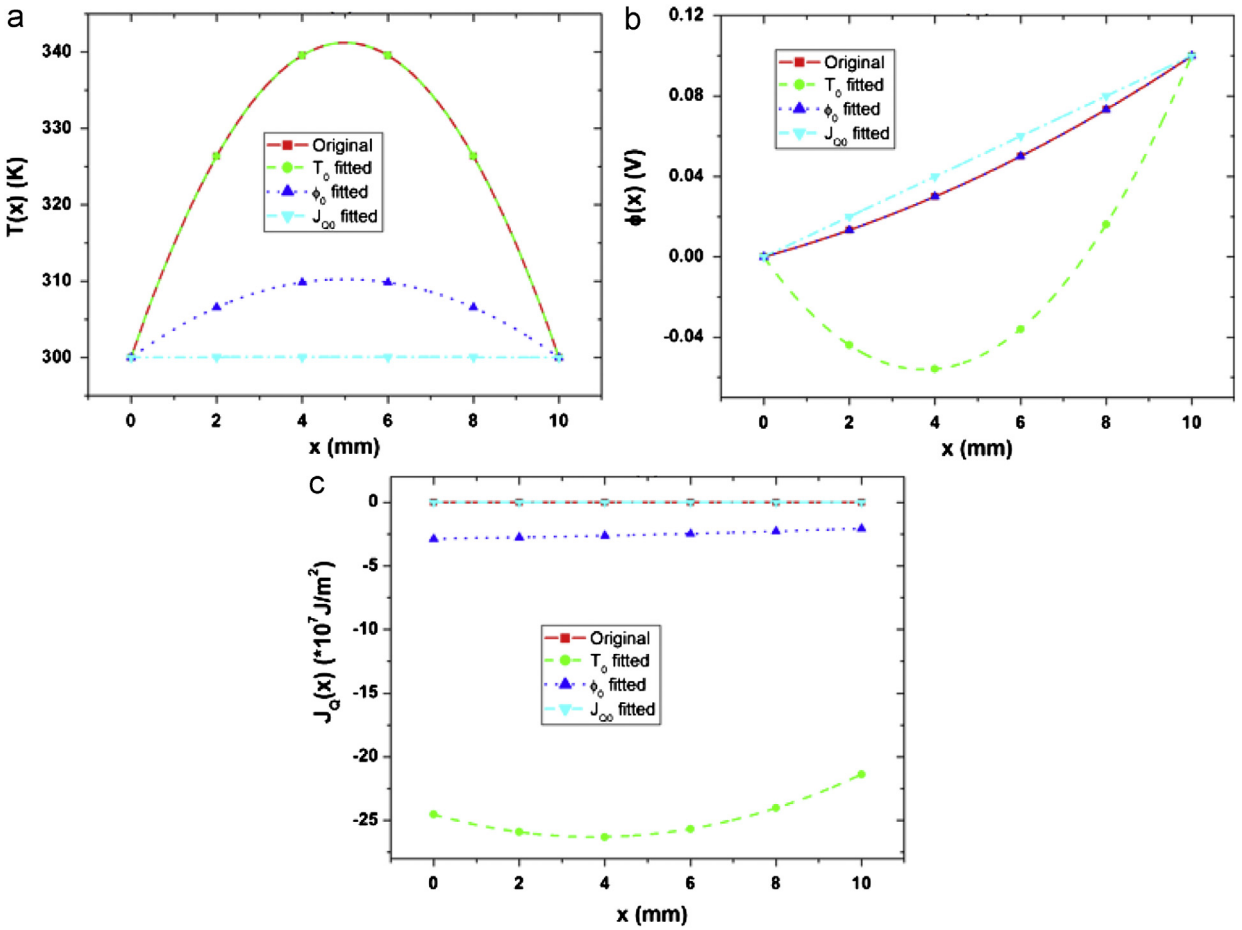

Fig. 6. Distribution of (a) temperature, (b) electric potential, and (c) heat flux of thermoelectric composite are fitted to the solutions of homogeneous material for $\phi(0)=0$, $\phi(L)=0.1$ V, $T(0)=T(L)=300$ K, and $f=0.4$.

dependence of the effective electric conductivity and figure of merit on boundary condition. We further calculated the optimized conversion efficiency of the composite versus the volume fraction of Bi_2Te_3 with $T(0)=800$ K and $T(L)=300$ K, as shown in Fig. 8, along with the conversion efficiency calculated using the effective figure of merit based on Eq. (69), and it is clear that there is a large discrepancy between the actual efficiency and the efficiency evaluated from the effective figure of merit, which depends on boundary condition. This suggests that the effective thermoelectric figure of merit of composite is not well defined, and does not correlate with its thermoelectric conversion efficiency.

The lack of correlation between the effective figure of merit and the thermoelectric conversion efficiency can be understood as following. To define the effective Seebeck coefficient, electric conductivity, and thermal conductivity, two sets of boundary conditions are required, making it impossible to match the actual optimal boundary condition under which the conversion efficiency is evaluated. This motivates us to suggest an alternative way to define the effective thermoelectric properties, using equivalency principle under optimal working condition in combination with the requirements of Eqs. (65) and (69) instead, and interestingly, this leads to two sets of effective properties, as shown in Fig. 9 along with the effective Z^*. This again suggests that the effective properties of thermoelectric composites are ill-defined.

6. Concluding remarks

In conclusion, we developed rigorous nonlinear asymptotic homogenization theory to analyze the coupled transport of electricity and heat in thermoelectric composite materials, with which we solved for the macroscopic field distributions that are drastically different from those in homogeneous materials, analyzed the overall conversion efficiency using an idealized thermoelectric module, and showed that the effective thermoelectric properties are ill-defined, and the effective thermoelectric figure of merit does not directly correlate with the thermoelectric conversion efficiency. The analysis thus sheds

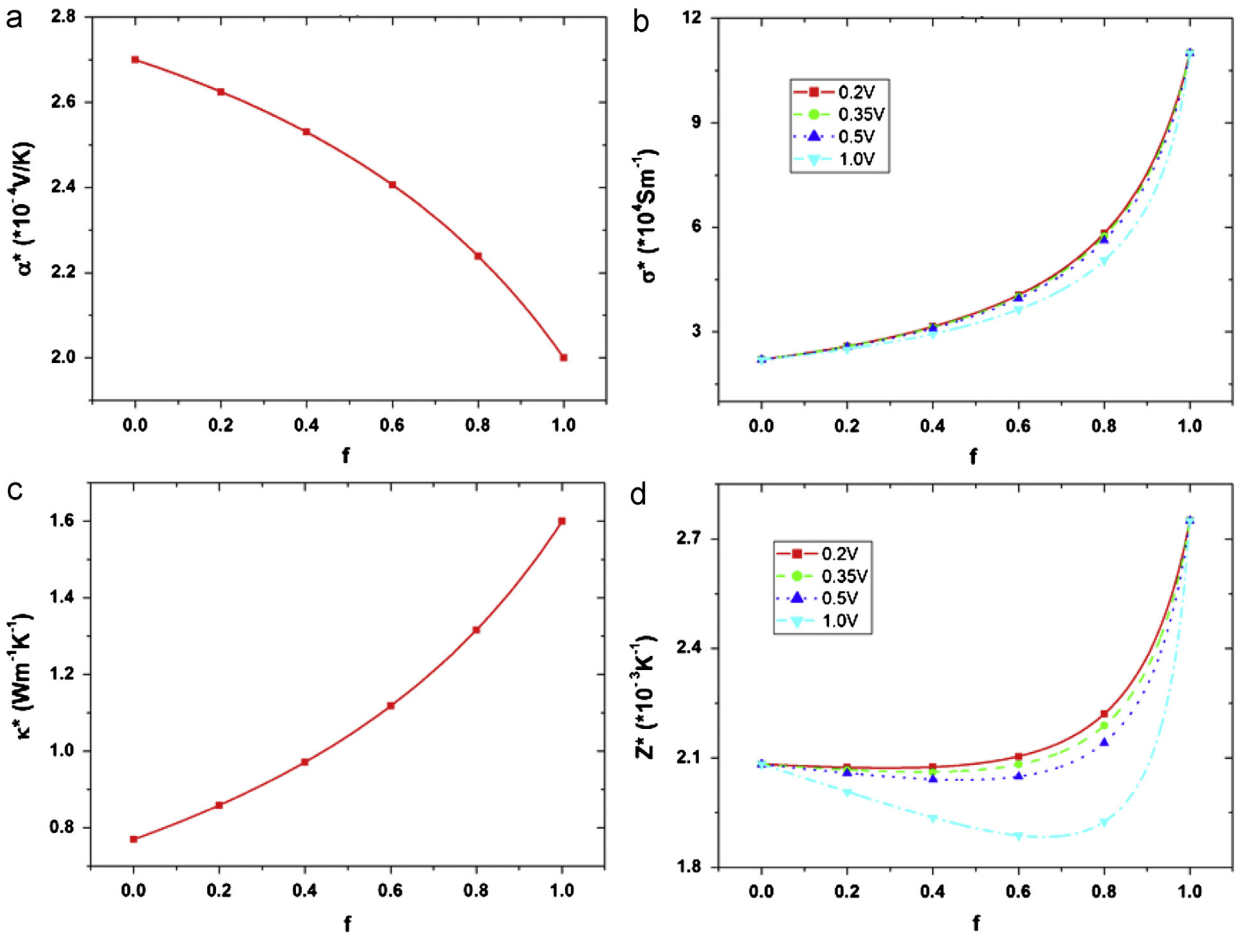

Fig. 7. The effective thermoelectric properties calculated by equivalency principle; (a) electric conductivity; (b) Seebeck coefficient; (c) thermal conductivity; and (d) figure of merit.

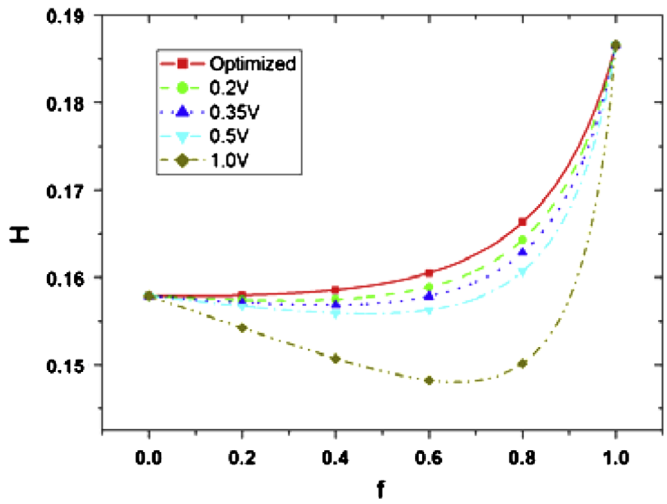

Fig. 8. Conversion efficiencies of composite versus volume fraction. There is a discrepancy between directly optimized value and the results converted from effective figures of merit from different boundary conditions.

considerable insight into the effective behavior of thermoelectric composites that can be used for their design and optimization.

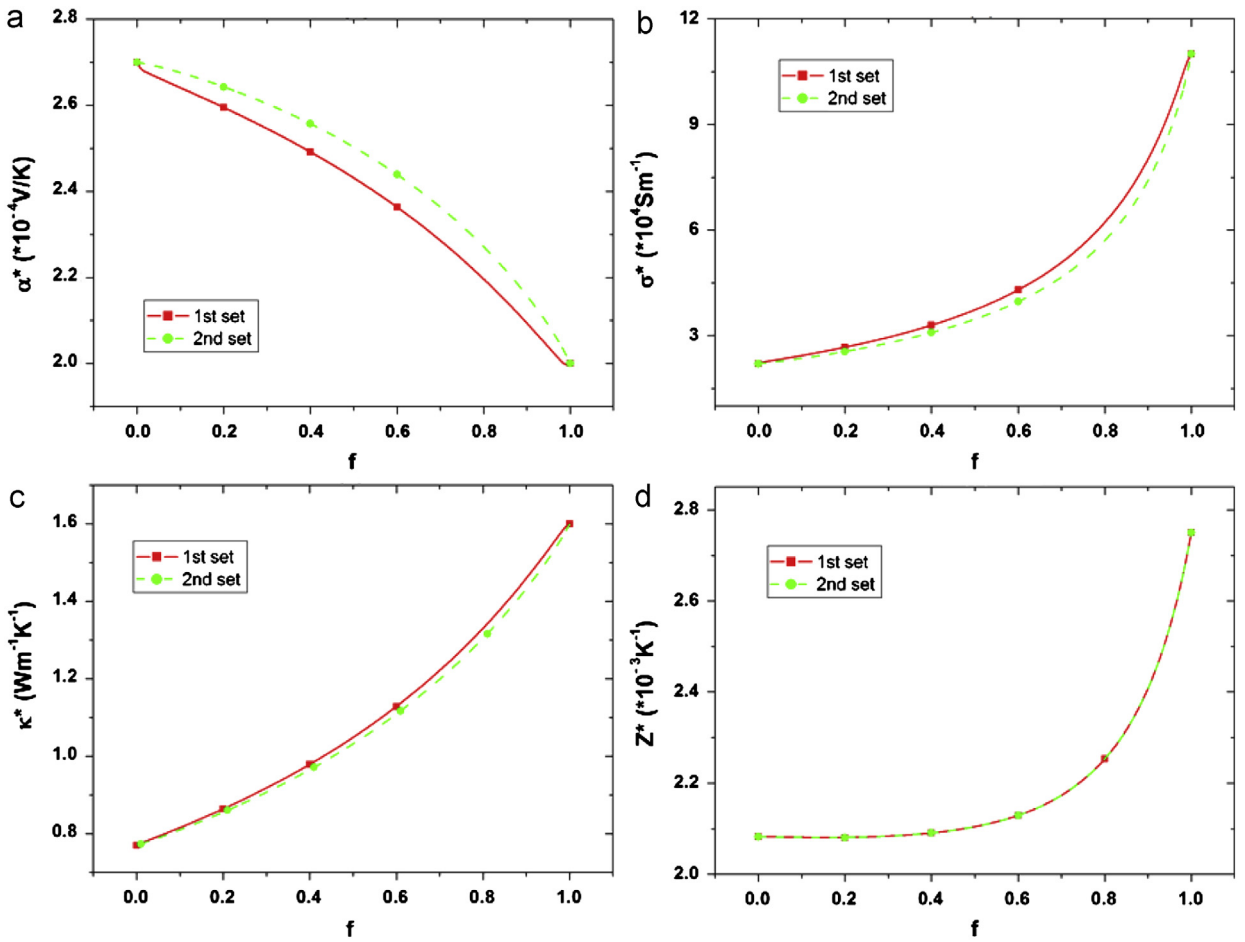

Fig. 9. Two sets of effective thermoelectric properties corresponding to a given conversion efficiency, evaluated at $T(L) = 300$ K, $T(0) = 1000$ K; (a) electric conductivity; (b) Seebeck coefficient; (c) thermal conductivity; and (d) figure of merit.

Acknowledgment

We gratefully acknowledge the support of AFOSR (FA9550-12-1-0325), NSF (CMMI-1235535), and NSFC (11172255).

References

Agoras, M., Lopez-Pamies, O., Castaneda, P.P., 2009. Onset of macroscopic instabilities in fiber-reinforced elastomers at finite strain. J. Mech. Phys. Solids 57, 1828–1850.

Alboni, P.N., Ji, X., He, J., Gothard, N., Tritt, T.M., 2008. Thermoelectric properties of La(0.9)CoFe(3)Sb(12)–CoSb(3) skutterudite nanocomposites. J. Appl. Phys. 103, 113707-1–113707-5.

Androulakis, J., Hsu, K.F., Pcionek, R., Kong, H., Uher, C., DAngelo, J.J., Downey, A., Hogan, T., Kanatzidis, M.G., 2006. Nanostructuring and high thermoelectric efficiency in p-Type Ag(Pb1-ySny)mSbTe2+m. Adv. Mater. 18, 1170–1173.

Antonova, E.E., Looman, D.C., 2005. Finite elements for thermoelectric device analysis in ANSYS. In: 24th International Conference on Thermoelectrics, 2005, ICT 2005, pp. 215–218.

Arachchige, I.U., Wu, J., Dravid, V.P., Kanatzidis, M.G., 2008. Nanocrystals of the quaternary thermoelectric materials: $AgPb_mSbTe_{m+2}$ ($m=1$–18): phase-segregated or solid solutions? Adv. Mater. 20, 3638–3642.

Bakhvalov, N.S., Panasenko, G.P., 1989. Homogenisation: Averaging Processes in Periodic Media: Mathematical Problems in the Mechanics of Composite Materials. Kluwer Academic Publishers.

Bell, L.E., 2008. Cooling, heating, generating power, and recovering waste heat with thermoelectric systems. Science 321, 1457–1461.

Bergman, D.J., Levy, O., 1991. Thermoelectric properties of a composite medium. J. Appl. Phys. 70, 6821–6833.

Bergman, D.J., Fel, L.G., 1999. Enhancement of thermoelectric power factor in composite thermoelectrics. J. Appl. Phys. 85, 8205–8216.

Callen, H.B., 1960. Thermodynamics; An Introduction to the Physical Theories of Equilibrium Thermostatics and Irreversible Thermodynamics. Wiley.

Cao, Y.Q., Zhao, X.B., Zhu, T.J., Zhang, X.B., Tu, J.P., 2008. Syntheses and thermoelectric properties of Bi(2)Te(3)/Sb(2)Te(3) bulk nanocomposites with laminated nanostructure. Appl. Phys. Lett. 92, 143106-1–143106-3.

Ghosh, S., Bai, J., Paquet, D., 2009. Homogenization-based continuum plasticity-damage model for ductile failure of materials containing heterogeneities. J. Mech, Phys. Solids 57, 1017–1044.

Gothard, N., Ji, X., He, J., Tritta, T.M., 2008. Thermoelectric and transport properties of n-type Bi_2Te_3 nanocomposites. J. Appl. Phys. 103, 054314-1–054314-4.

Goupil, C., Seifert, W., Zabrocki, K., Muller, E., Snyder, G.J., 2011. Thermodynamics of thermoelectric phenomena and applications. Entropy 13, 1481–1517.

Hao, F., Fang, D.N., Li, J.Y., 2012. Thermoelectric transport in heterogeneous medium: the role of thermal boundary resistance. Eur. Phys. J. Appl. Phys. 58, 58–30901.
Hashin, Z., Shtrikman, S., 1962. A variational approach to the theory of the effective magnetic permeability of multiphase materials. J. Appl. Phys. 33, 3125–3131.
Heremans, J.P., Thrush, C.M., Morelli, D.T., Wu, M.C., 2002. Thermoelectric power of bismuth nanocomposites. Phys. Rev. Lett. 88, 216801-1–216801-4.
Homentcovschi, D., Dascalu, C., 2000. Uniform asymptotic solutions for lamellar inhomogeneities in plane elasticity. J. Mech. Phys. Solids 48, 153–173.
Kalamkarov, A.L., Hassan, E.M., Georgiades, A.V., Savi, M.A., 2009. Asymptotic homogenization model for 3D grid-reinforced composite structures with generally orthotropic reinforcements. Compos. Struct. 89, 186–196.
Ke, X.Z., Chen, C.F., Yang, J.H., Wu, L.J., Zhou, J., Li, Q., Zhu, Y.M., Kent, P.R.C., 2009. Microstructure and a nucleation mechanism for nanoprecipitates in PbTe-AgSbTe2. Phys. Rev. Lett. 103, 145502-1–145502-4.
Kim, H.J., Bozin, E.S., Haile, S.M., Snyder, G.J., Billinge, S.J.L., 2007. Nanoscale alpha-structural domains in the phonon-glass thermoelectric material beta-Zn_4Sb_3. Phys. Rev. B 75, 134103-1–134103-4.
Kraemer, D., Poudel, B., Feng, H.P., Caylor, J.C., Yu, B., Yan, X., Ma, Y., Wang, X.W., Wang, D.Z., Muto, A., McEnaney, K., Chiesa, M., Ren, Z.F., Chen, G., 2011. High-performance flat-panel solar thermoelectric generators with high thermal concentration. Nat. Mater. 10, 532–538.
Lin, H., Bozin, E.S., Billinge, S.J.L., Quarez, E., Kanatzidis, M.G., 2005. Nanoscale clusters in the high performance thermoelectric AgPbmSbTem+2. Phys. Rev. B 72, 174113-1–174113-7.
Liu, L.P., 2012. A continuum theory of thermoelectric bodies and effective properties of thermoelectric composites. Int. J. Eng. Sci. 55, 35–53.
Milgrom, M., Shtrikman, S., 1989. Linear response of two-phase composites with cross moduli: exact universal relations. Phys. Rev. A 40, 1568–1575.
Milton, G.W., 2002. The Theory of Composites. Cambridge University Press.
Narducci, D., 2011. Do we really need high thermoelectric figures of merit? A critical appraisal to the power conversion efficiency of thermoelectric materials. Appl. Phys. Lett. 99, 102104-1–102104-3.
Pei, Y.Z., Lensch-Falk, J., Toberer, E.S., Medlin, D.L., Snyder, G.J., 2011. High thermoelectric performance in PbTe due to large nanoscale Ag-2 Te precipitates and La doping. Adv. Funct. Mater. 21, 241–249.
Poudel, B., Hao, Q., Ma, Y., Lan, Y.C., Minnich, A., Yu, B., Yan, X.A., Wang, D.Z., Muto, A., Vashaee, D., Chen, X.Y., Liu, J.M., Dresselhaus, M.S., Chen, G., Ren, Z.F., 2008. High-thermoelectric performance of nanostructured bismuth antimony telluride bulk alloys. Science 320, 634–638.
Poudeu, P.F.P., Gueguen, A., Wu, C.I., Hogan, T., Kanatzidis, M.G., 2010. High figure of merit in nanostructured n-type KPbmSbTem+2 thermoelectric materials. Chem. Mater. 22, 1046–1053.
Tarn, J.Q., 1997. An asymptotic theory for nonlinear analysts of multilayered anisotropic plates. J. Mech. Phys. Solids 45, 1105–1120.
Triantafyllidis, N., Bardenhagen, S., 1996. The influence of scale size on the stability of periodic solids and the role of associated higher order gradient continuum models. J. Mech. Phys. Solids 44, 1891–1928.
Tritt, T.M., Subramanian, M.A., 2006. Thermoelectric materials, phenomena, and applications: a bird's eye view. MRS Bullet. 31, 188–194.
Tritt, T.M., Boettner, H., Chen, L., 2008. Thermoelectrics: direct solar thermal energy conversion. MRS Bullet. 33, 366–368.
Vashaee, D., Shakouri, A., 2004. Improved thermoelectric power factor in metal-based superlattices. Phys. Rev. Lett. 92, 106103-1–106103-4.
Webman, I., Jortner, J., Cohen, M.H., 1977. Thermoelectric-power in inhomogeneous materials. Phys. Rev. B 16, 2959–2964.
Xie, W.J., Tang, X.F., Yan, Y.G., Zhang, Q.J., Tritt, T.M., 2009. Unique nanostructures and enhanced thermoelectric performance of melt-spun BiSbTe alloys. Appl. Phys. Lett. 94, 102111-1–102111-3.
Xie, W.J., He, J., Kang, H.J., Tang, X.F., Zhu, S., Laver, M., Wang, S.Y., Copley, J.R.D., Brown, C.M., Zhang, Q.J., Tritt, T.M., 2010. Identifying the specific nanostructures responsible for the high thermoelectric performance of (Bi,Sb)(2)Te-3 nanocomposites. Nano Lett. 10, 3283–3289.
Yang, J.H., Caillat, T., 2006. Thermoelectric materials for space and automotive power generation. MRS Bullet. 31, 224–229.
Yang, Y., Xie, S.H., Ma, F.Y., Li, J.Y., 2012. On the effective thermoelectric properties of layered heterogeneous medium. J. Appl. Phys. 111, 013510-1–013510-7.
Yang, Y., Ma, F.Y., Lei, C.H., Liu, Y.Y., Li, J.Y., 2013. Is thermoelectric conversion efficiency of a composite bounded by its constituents? Appl. Phys. Lett. 102, 053905-1–053905-4.
Zhou, M., Li, J.F., Kita, T., 2008. Nanostructured AgPbmSbTem+2 system bulk materials with enhanced thermoelectric performance. J. Am. Chem. Soc. 130, 4527–4532.
Zhu, G.H., Lee, H., Lan, Y.C., Wang, X.W., Joshi, G., Wang, D.Z., Yang, J., Vashaee, D., Guilbert, H., Pillitteri, A., Dresselhaus, M.S., Chen, G., Ren, Z.F., 2009. Increased phonon scattering by nanograins and point defects in nanostructured silicon with a low concentration of germanium. Phys. Rev. Lett. 102, 196803-1–196803-4.